Optical properties of $PbTiO_3$, $PbZr_xTi_{1-x}O_3$, and $PbZrO_3$ films deposited by metalorganic chemical vapor on $SrTiO_3$

M. P. Moret, M. A. C. Devillers, K. Wörhoff, and P. K. Larsen

Citation: Journal of Applied Physics **92**, 468 (2002); doi: 10.1063/1.1486048
View online: https://doi.org/10.1063/1.1486048
View Table of Contents: http://aip.scitation.org/toc/jap/92/1
Published by the American Institute of Physics

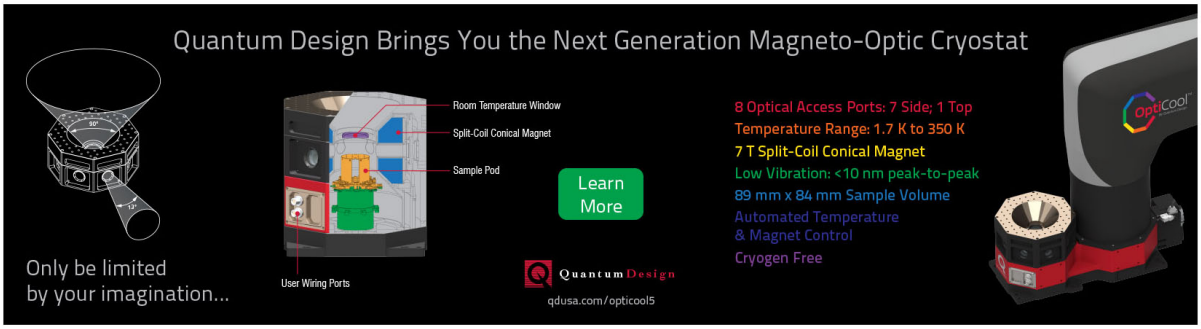

Optical properties of $PbTiO_3$, $PbZr_xTi_{1-x}O_3$, and $PbZrO_3$ films deposited by metalorganic chemical vapor on $SrTiO_3$

M. P. Moret[a] and M. A. C. Devillers
University of Nijmegen, Research Institute for Materials, Toernooiveld 1, 6525 ED Nijmegen, The Netherlands

K. Wörhoff
University of Twente, MESA+ Research Institute, P.O. Box 217, 7500 AE Enschede, The Netherlands

P. K. Larsen
University of Nijmegen, Research Institute for Materials, Toernooiveld 1, 6525 ED Nijmegen, The Netherlands

(Received 20 December 2001; accepted for publication 22 April 2002)

Epitaxial $PbZr_xTi_{1-x}O_3$ (PZT) films have been prepared by metalorganic chemical vapor deposition on $SrTiO_3$ substrates. Two sets of films of thicknesses 50–100 and 700–1400 nm, containing 0%, 40%, 60%, and 100% Zr, were prepared and investigated. The refractive index n was determined by ellipsometry for the thin films and by reflectivity for the thicker films. Results were obtained over the energy range from 1.55 to 3.72 eV, and with a Cauchy-fit extrapolation down to 0.62 eV. The refractive-index curves show a systematic variation with composition. For all compositions, n is close to 3.2 at 3.72 eV (333 nm), while at 1.55 eV (800 nm) n is 2.35 for PZ ($x=1$) and 2.61 for PT ($x=0$). In agreement with previous results we find that the optical band gap is essentially independent of composition for PZT. We obtained 3.6 ± 0.1 eV. The $n(E)$ results were analyzed by a Wemple–DiDomenico dispersion analysis, yielding results for the dispersion region in the ultraviolet. Unlike the band gap, which is insensitive to composition in PZT, the dispersion energy E_d decreases from PT to PZ in the same fashion as the refractive index in the transparent region.
 [DOI: 10.1063/1.1486048]

I. INTRODUCTION

Ferroelectric films have attracted quite a lot of attention as memories and piezoelectric devices.[1] Though they also can be used as electro–optical devices in nonlinear optic applications[2] or in electro–optic modulators,[3,4] there are relatively few reports of such applications. Bulk ceramics are already used, but films are more advantageous as waveguide electro–optic modulators require relatively low drive power in comparison to bulk modulators. Moreover, thin films are more readily integrated in existing semiconductor technologies than bulk hybrid technologies. Ferroelectric films for waveguide-modulator applications should have low optical loss and low roughness for waveguiding and a high electro–optic coefficient for the refractive-index modulation. Though epitaxial films can fulfill these criteria, their growth is difficult and only small crystals are available as substrates. The long-term goal in this area is the production of high-quality epitaxial films on large diameter silicon-based substrates, since such films would offer a large surface for growth and device development. Recently, GaAs has been grown on Si using an intermediate thin film of $SrTiO_3$ (STO).[5] Such silicon-supported STO and MgO[6] films may be used in the future as substrates for oxide ferroelectric films.

$PbZr_xTi_{1-x}O_3$ (PZT) is a family of oxide ferroelectrics under active consideration for optical applications as their properties are strongly dependent on x, where $x(0\leqslant x\leqslant 1)$ is the zirconium fraction ($x=[\mathrm{Zr}]/([\mathrm{Zr}]+[\mathrm{Ti}])$. Near the tetragonal/rhombohedral phase transition for x around 0.53, anomalously high dielectric constants have been measured and high electro–optic coefficients are expected. Detailed optical studies are available on $Pb_{1-y}La_yZr_xTi_{1-x}O_3$ (PLZT) ceramics,[3,7] but optical and dispersion data for thin films as a function of the x ratio are scarce. Three articles were found on PLZT ceramics and sol–gel films[8–10] and two on metal-organic chemical vapor deposition (MOCVD) PZT films.[11,12]

In this article, we report on the optical properties of PZT films grown by MOCVD on STO. The PZT film composition studied spanned the full composition range from PT ($x=0$) to PZ ($x=1$). Thin films of thicknesses 50–100 nm and thick films of thicknesses 700–1400 nm were grown by MOCVD. Wavelength-dependent ellipsometry and reflectivity measurements were carried out to investigate the optical properties of the films in the transparent region below the band gap, from 3.72 eV (333 nm) in the near ultraviolet to 1.55 eV (800 nm) in the red. Cauchy extrapolation was used to estimate the refractive index down to 0.62 eV (2000 nm) in the infrared. A Wemple–DiDomenico single-oscillator dispersion analysis was carried out to quantitatively characterize the observed refractive-index behavior. Finally, light could be coupled in two PZT ($x=0.6$) films by prism coupling confirming their high degree of optical quality.

[a]Author to whom correspondence should be addressed; electronic mail: mona@sci.kun.nl

TABLE I. List of samples studied.

Composition	Thickness (nm)	rms top-surface roughness (nm)
$PbTiO_3$	50±5	4.2±1.3
$PbZr_{0.4}Ti_{0.6}O_3$	90±5	0.55±0.01
$PbZr_{0.6}Ti_{0.4}O_3$	94±5	0.89
$PbZrO_3$	105±5	0.57
$PbZr_{0.6}Ti_{0.4}O_3$	340±10	0.59±0.01
$PbTiO_3$	790±10	4.17
$PbZr_{0.4}Ti_{0.6}O_3$	800±10	0.93
$PbZr_{0.6}Ti_{0.4}O_3$	700±10	1.05
$PbZrO_3$	1420±30	45.3
$PbZrO_3$ dry etched	1260±30	18.4

II. EXPERIMENT

A. Epitaxial PZT films

The PZT thin films were grown by MOCVD at 700 °C in a cold-wall horizontal-flow reactor equipped with a rotating susceptor and heated by infrared lamps. Tetraethyllead ($Pb(C_2H_5)_4$), zirconium tetra-*t*-butoxide $Zr(OC(CH_3)_3)_4$, and titanium tetra-*t*-butoxide $Ti(OC(CH_3)_3)_4$ were used as precursors, oxygen as the oxidizing agent, and nitrogen as the carrier gas. The films were examined as a function of the Zr/(Zr+Ti) ratio in the gas phase by varying the Zr flow with respect to the Ti flow keeping the total species quantity constant. STO substrates, 0.5 mm thick, (001) crystals oriented within ±0.5° were used. For the thin films the substrate surface dimensions were 20 mm diameter and 1 by 1 cm for the thick films. The substrates were cleaned successively in acetone, isopropanol, and demineralized water prior to growth.

The structure of the films was investigated by x-ray diffraction using a Bruker D8 Discovery x-ray diffractometer with a Cu target ($\lambda = 1.54060$ Å) and a four-bounce monochromator Ge (022). This instrument was also used to carry out x-ray reflectivity measurements on the PZT films. This allows a determination of the film thickness up to 200–300 nm. The thicknesses of all the films were estimated by weighting the substrate prior to and after growth and confirmed by ellipsometry for all films and by transmission electron microscope (TEM) cross sections for the thick films. The surface morphology of the films was investigated with a Digital Instruments atomic force microscope (AFM) Dimension 3100 in contact mode. The composition of the samples was analyzed by x-ray fluorescence (XRF) and by energy dispersive spectroscopy (EDS) in the TEM. In Table I, the composition, thickness, and surface roughness of the PZT films grown by MOCVD on STO substrates are shown. The as-grown surface quality varies as a function of composition due to differences in growth mechanisms depending on the Zr content in the films. The thin PT films have a higher roughness as they have a more island-type growth, confirmed by the 50 nm PT layer not yet continuous. On the other hand, the thick PT films also have a rms of ~4 nm but this is caused by the presence of *a*- and *c*-domain structures, rather than by a discontinuous layer. Zr-containing thin films are smoother than the PT films and continuous. However the thick PZ film surface is very rough as the layer is terminated by ~250 nm high PZ pyramids.[13] The PZ film roughness could be decreased by a factor of 2.5 by dry etching. The roughness of the thick PZT films ($x = 0.4, 0.6$) is well within the waveguide device requirements (see Table I), and PZT($x = 0.6$) (rhombohedral phase) films were used for prism-coupling experiments. Further details on growth and structure of the films will be published later.

B. Ellipsometry

Ellipsometry measurements were performed with a Gaertner L117C ellipsometer using a HeNe laser at 633 nm. The measurements of the ellipsometric angles Δ and Ψ were carried out at room temperature (RT) at 70° angle of incidence. A home-built system similar to a rotating analyzer ellipsometer was used for the wavelength-dependent ellipsometry measurements. Typical resolution for an ellipsometry measurement with an ideal specular reflecting and homogenous sample are $\Psi \pm 0.005°$ and $\Delta \pm 0.05°$. Ellipsometry was used to measure the refractive index of the films and then estimate the composition (x) of the PZT from the refractive index.

On the basis of published values of the refractive index versus PZT composition[8,11] as well as on the basis of our own measurements presented in this study, we calculated (Δ, Ψ) contours for a number of PZT compositions on STO substrates using a linear extrapolation between the refractive index and the x ratio with $n_{PT} = (2.66,0.0)$ and $n_{PZ} = (2.46,0.0)$ at $\lambda = 633$ nm. Such contours are shown in Fig. 1 as a function of thickness for several PZT compositions. For the compositions shown in Fig. 1(a), the curves are ''degenerate'' as the path is the same for different thicknesses. If an interface layer or a top-surface roughness is introduced, the curves become ''nondegenerate'' as the (Δ, Ψ) contours can split or shift considerably and become different for different thicknesses. This is shown in Fig. 1(b) using the same interface and surface layers for the three different compositions with $n_{interface} = (2.45,0.0)$ and $n_{surface} = (1.80,0.0)$ representing respectively, approximately 50% STO–50% PZT ($x = 0.5$) and 50% PZT ($x = 0.5$)–50% air, using $n_{STO} = (2.39,0.0)$ at $\lambda = 633$ nm as given in Ref. 14. The nondegeneracy introduces extra difficulty in determining the exact refractive index of the layer, especially for the compositions shown in Fig. 1(b) where the curves are very close to each other. One measurement is often not enough to obtain unambiguous information.

In our work, we have made use of the fact that the growth conditions across the 4 in. diam susceptor during a MOCVD growth run are not radially homogeneous. By growing PZT layers simultaneously on a number of substrates placed on the susceptor in the same growth run, we were able to measure the PZT films of different thickness and composition. A (interface roughness/film/top roughness) model was used to fit the ellipsometry data using the same values for the refractive indices of the interface and top roughness layers as described above for Fig. 1. The thicknesses obtained from the three-layer model were systematically verified. The rms top-surface roughness of the layer

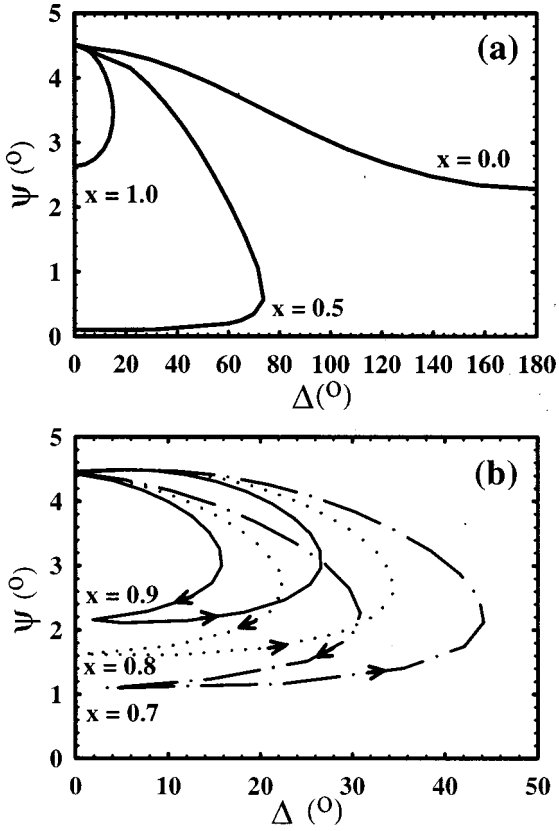

FIG. 1. Calculated ellipsometry (Δ, Ψ) contours as a function of thickness at $\lambda = 633$ nm at $\varphi = 70°$ for several $x = [\mathrm{Zr}]/[\mathrm{Zr}+\mathrm{Ti}]$ ratios. The curves bounce back and forth every ~60 nm with the arrows indicating the increasing thickness direction on the contours: (a) for $x = 1.0$, 0.5, 0.0 with no interface and no top roughness using 2.46, 2.56, and 2.66 as the respective values of the real part of the refractive index for these three compositions; (b) for $x = 0.9$, 0.8, 0.7 with 1 nm interface and 1 nm top roughness. The respective values of the real part of the refractive index are 2.48, 2.50, and 2.52. The same values 2.45 and 1.80 of the refractive index were used, respectively, for the interface and the surface layers for the three compositions.

was measured for all layers by AFM (Table I). The rms top-surface roughness, measured by AFM, coincides well with the top-surface roughnesses from the ellipsometry model, corresponding more to a peak-to-peak value. The thicknesses of the films were confirmed by other means as mentioned earlier (e.g., by x-ray reflectivity for the thin layers[15] and by optical reflectivity for the thick films). We determined the real part of the refractive index n with an error of ± 0.01. The absorption coefficient k was assumed to be zero. In all calculations the film anisotropy was neglected. Earlier studies reported the birefringence of PT films grown on MgO ($5 \pm 3\times10^{-3}$) and of PT crystals ($\approx 9\times10^{-3}$).[12]

C. Reflectivity

The refractive index dispersion of the thicker films was determined by optical reflectivity (using a xenon lamp at 150 W) with *s*-polarized light on the wavelength dependent ellipsometer described in the previous section. The resolution is estimated to be $\Delta\lambda \approx 1$ nm. The thick films were more easily measured by reflectivity than ellipsometry due to the smaller sensitivity to surface roughness for reflectivity. The reflectivity was measured as a function of wavelength from 300 to 800 nm. The obtained interference fringes were indexed by plotting N (fringe number) as a function of $1/\lambda$ through the origin and calibrating the refractive index at 633 nm using the ellipsometry measurement on the Gaertner. The dispersion of the refractive index could then be extracted. The band gap E_g of STO is about 3.2 eV[14] and is lower than that of PZT ceramics,[8] therefore direct band gap determination of our PZT films by transmission measurements was not possible and the reflectivity measurements, on the thick films, were performed to measure the band gap of the films (Fig. 2, zone 1). We estimated the band gap as the photon energy at which, with increasing photon energy, the interference

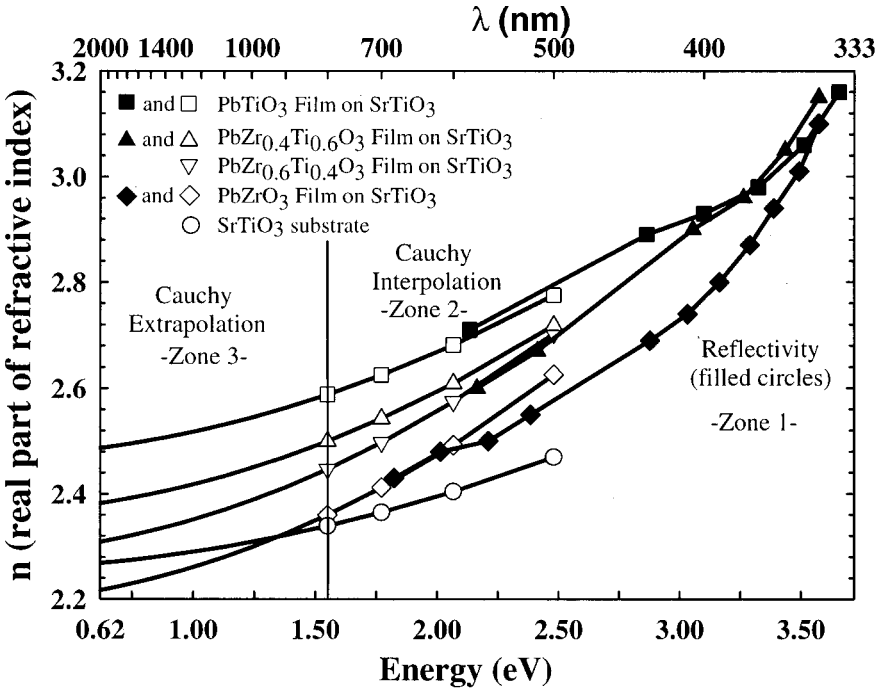

FIG. 2. The refractive index of PZT as a function of composition and wavelength. Zone 1 contains the results of the reflectivity measurements (filled symbols). Zone 2 contains the results of the ellipsometry measurements (open symbols). The curves in zone 2 are Cauchy interpolations based on the experimental points. The curves in zone 3 are Cauchy extrapolations into the infrared.

TABLE II. Refractive index values (at RT) of PZT ceramics and films.

Film	λ (nm); *n*	Technique	Reference
PLZT (8/100/0) ceramics	633; 2.42	Ellipsometry	8
PLZT (8/80/20) ceramics	633; 2.479		
PLZT (2/65/35) ceramics	633; 2.523		
PLZT (16/40/60) ceramics	633; 2.552		
PLZT (8/10/90) ceramics	633; 2.644		
PLZT (0/0/100) ceramics	633; 2.668		
Sol–gel PT	633; ≈2.58	Transmittance	9
Sol–gel PZT 40/60	633; ≈2.45		
Sol–gel PZT 60/40	633; ≈2.40		
Sol–gel PZ	633; ≈2.30		
MOCVD PT on STO	633; ≈2.675	Prism	11
MOCVD PZT (20/80)on STO	633; ≈2.607	coupling	
MOCVD PZT (80/20)on STO	633; ≈2.505		
MOCVD PZ on STO	633; ≈2.46		
MOCVD PT on STO	633; ≈2.67 450; ≈2.85	Prism coupling	12
Film PZT (*x*?) on $LaNiO_3$ /$LaAlO_3$	400–800; 2.25–2.2	Reflectance	16
Sol–gel PZT (50/50) on platinized Si	650; ≈1.9	Ellipsometer	17
Sputtered PZT (25/75) on platinized Si	400; 2.875 500; 2.65	Ellipsometry	18
Sputtered PZT50/50 on (1–102) and on (0001) sapphire	633; 2.44 633; 2.54	Ellipsometry	20

fringes abruptly disappeared (showing that the film was no longer transparent). For a film with a thickness of 700 nm, this occurs at an absorption coefficient of about 30 000 cm^{-1}. At this high level of optical absorption, impurities are unlikely to have an appreciable influence, so that this procedure for estimating the band gap is reasonable.

III. RESULTS AND DISCUSSION

A. Refractive index

Refractive indices for specific PZT compositions are available from the literature (Table II). The values in Table II are from films prepared by different techniques and from bulk ceramics, and some reports indicate a different refractive index for thin films than for ceramics.[9,16–18] Optical characterization can be used as a quality check for PZT films. In Ref. 9, the linear variation of the refractive index, from PT to PZ, was used to determine the packing densities of the films. The lower refractive index [roughly 5% lower than for ceramics[8] or MOCVD films (our data)] is due to a 95% packing density of the sol–gel films. Similar results were found for sol–gel PLT films.[10] In Ref. 19, the increase of the refractive index with increasing annealing time was monitored for sol–gel films. The differences in the refractive index values (for samples with the same composition) result from variations in the details of the film structure (phase, interface, inhomogeneity, domains, microstructure, top roughness) and how these parameters were taken into account in the data analysis.

Figure 2 presents our results for the dispersion of the refractive index of PZT. There are three different zones in the dispersion curves of the refractive index. Zone 1 shows the refractive index of the thick films as measured by reflectivity on thick films (filled symbols). Zone 2 is the refractive index as measured by ellipsometry on thin films at wavelengths of 500, 600, 700, and 800 nm (open symbols). The values of the refractive index are in very good agreement at 633 nm with reported values.[8,11,12,20] The zone-2 data were fitted by a Cauchy fit of the form

$$n(\lambda) = n_0 + a\left(\frac{800}{\lambda}\right)^2.$$

A fit in $1/\lambda^2$ was found to be sufficient to extrapolate the data (zone 3) up to 2000 nm. The fit coefficients n_0 and a, shown in Table III for the different compositions, are listed indicatively as they do not represent any physical quantities as the parameters of the other fit used below.

As mentioned in Sec. I, few references reporting the refractive-index variation as a function of composition were found in the literature. An early article on PLZT ceramics[8] showed that the refractive index decreases linearly from PT ($n=2.66$) to PZ ($n=2.46$) at $\lambda=633$ nm. Similar results

TABLE III. Coefficients of the Cauchy fit for zones 2 and 3 in Fig. 2.

Composition	n_0	a
$PbTiO_3$	2.468	0.120
$PbZr_{0.4}Ti_{0.6}O_3$	2.360	0.140
$PbZr_{0.6}Ti_{0.4}O_3$	2.283	0.164
$PbZrO_3$	2.190	0.170
$SrTiO_3$	2.255	0.084

TABLE IV. Comparison of the dispersion of the refractive index for ceramics[a] and for our MOCVD films on STO.

	$PbZrO_3$		PLZT 10/65/35	PZT (60/40)	$PbTiO_3$	
Wavelength	Ref. 8	films	Ref. 8	films	Ref. 8	films
450	2.56	2.66	2.64	2.76	—	2.86
500	2.50	2.60	2.58	2.66	2.78	2.82
600	2.46	2.50	2.50	2.60	2.70	2.70
700	2.44	2.41	2.46	2.52	2.66	2.62

[a]See Ref. 8.

were later found for MOCVD PZT films.[11] The measurements are in agreement at 633 nm for MOCVD films and ceramics but the reference on MOCVD films does not contain dispersion data. In Ref. 8, it is also shown that the La content has little influence on the refractive index, which is determined mainly by x. Initially the linear extrapolation of the refractive index as a function of x was used to determine the composition of our PZT films.[15] The composition determination by ellipsometry was possible using the determination of the real part of the refractive index n, with ± 0.01 error, leading to ± 0.1 error in the x ratio. The composition estimation by ellipsometry is in good agreement with chemical analysis by XRF and EDS (TEM). The four compositions of PZT in zone 2 also indicate a linear decrease of n from PT (2.66) to PZ (2.46) at 633 nm for our films. It is only measured for four PZT compositions and large variation might be expected around the morphotropic phase boundary due to the eventual presence of two phases in the film, or possibly even three.[21] The linear variation of the refractive index from PT to PZ is preserved up to 2000 nm according to the Cauchy extrapolation. The linear relation (n to x) preservation is important for electro–optics devices, which function at 1500 nm.

B. Band gap (E_g) and dispersion energy (E_d)

In Fig. 2 (zone 1), all the $n(E)$ curves converge near the absorption edge at 3.6 ± 0.1 eV (340 ± 10 nm), which compares well with the convergence observed near 350 nm for the ceramics[8] (Table IV). Good agreement had also been found between ceramics and PZT films on sapphire[20] over the wavelength range from 400 to 750 nm. In Ref. 12, a good match between MOCVD films and single crystals was reported for PT from $\lambda = 450$ to 635 nm. In Fig. 2, the reflectivity and the ellipsometry results are consistent in the overlap region. For clarity, only the reflectivity results for PT, PZT($x = 0.4$), and PZ are shown.

While the refractive index varies systematically as a function of x, no absorption-edge variation was found as a function of composition. In Table V, reported band gap values for PZT are listed. Our estimation of the gap is in reasonable agreement with previous ceramics estimates[8] and differ from film estimates.[9,16,22] The insensitivity of band gap to composition is consistent with results in Ref. 8, but in disagreement with Ref. 9. The endpoint values of the band gap variation claimed in Ref. 9 fall within our measured 3.6 ± 0.1 eV. No PZT composition determination is therefore possible by band-gap determination.

TABLE V. Band gap values for PZT.

Film	Band gap (eV)	Technique	Reference
MOCVD PT to PZ	3.6 ± 0.1 eV	Reflectivity	This work
Ceramics PLZT	≈3.5	Ellipsometry	8
Sol–gel PT Sol–gel PZT 40/60 Sol–gel PZT 60/40 Sol–gel PZ	≈3.45 ≈3.60 ≈3.65 ≈3.70	Transmittance	9
Film PZT (×?)on $LaNiO_3$ /$LaAlO_3$	3.07	Reflectance	16
Sol–gel PZT (65/35)	Main absorption at 3.37 eV and two secondary at 2.6 and 1 eV	Transmittance/ reflection	22

In addition to the Cauchy extrapolation described above, which was done to provide reasonable values for n in the infrared region, we have also carried out a Wemple–DiDomenico single-oscillator dispersion analysis using all of the experimental data of Fig. 2. Both Cauchy and Wemple–DiDomenico fits provide useful parametrizations of the experimental results. But the Wemple–DiDomenico fit additionally provides physically significant quantities, which characterize the strong interband-transition absorption band in the ultraviolet that causes the refractive-index dispersion in the visible. The widely used Wemple–DiDomenico dispersion relation[23] for $n(E)$, the refractive index at photon energy E is

$$n(E)^2 - 1 = \frac{E_d E_0}{(E_0^2 - E^2)}, \tag{1}$$

where E_0 is the energy of the effective dispersion oscillator, which is expected to correspond to the photon-energy position of the center of gravity of the ultraviolet band. E_d, called the dispersion energy, is a measure of the average strength of the interband optical transitions. Wemple–DiDomenico fits to the experimental data of Fig. 2 yield the estimates shown in Table VI. This table also includes, for discussion, the refractive index value at 1.55 eV (800 nm) in the transparent region.

The usual situation in insulators and semiconductors is to find an inverse correlation between the refractive index and the characteristic interband energy E_0. In semiconductors, this correlation works very well, and even extends to an

TABLE VI. Wemple–DiDomenico dispersion parameters for our MOCVD $Pb(Zr,Ti)O_3$ films.

MOCVD film	E_0	E_d	n(1.55 eV)
$PbTiO_3$	4.67	25.1	2.59
$PbZr_{0.4}Ti_{0.6}O_3$	4.27	20.7	2.50
$PbZr_{0.6}Ti_{0.4}O_3$	4.10	18.6	2.45
$PbZrO_3$	4.09	17.3	2.36

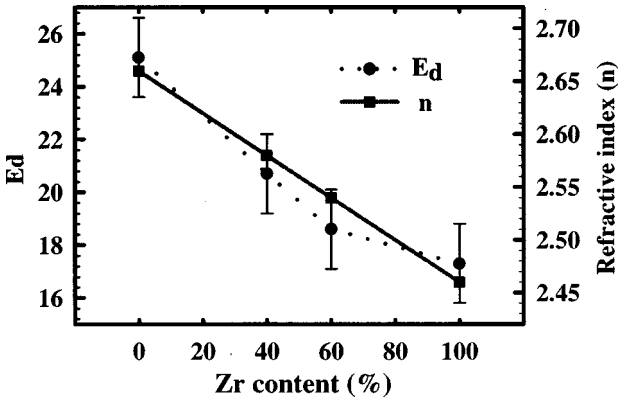

FIG. 3. The interband strength parameter E_d from the Wemple fit and the refractive index n at $\lambda = 633$ nm as a function of Zr content.

analogous correlation with the band gap energy[24] because the band gap in semiconductors is closely correlated with E_0. But in PZT, we find the surprising result that the transparent-region refractive index is not inversely correlated with E_0, which decreases slightly from PT to PZ. Instead, the behavior is dominated by the very strong composition dependence of the absorption-strength parameter E_d. We therefore conclude that the larger refractive index in PT arises primarily from stronger interband transitions in this material, rather than from a significant difference in interband energies between PT and PZ. This conclusion is also consistent with the finding that there is little difference between the band gaps of PT and PZ.

A 30% decrease in E_d from PT to PZ is found. If an error of ± 1.5 eV (which is reasonable considering the data) is taken for E_d, there is a nearly linear decrease in E_d as a function of decreasing x. The relationship E_d to x is very similar to the one for the refractive index (n) to x in the transparent regime, as shown in Fig. 3. Table VII shows reported values of the Wemple–DiDomenico E_d and E_0 for PLZT ceramics.[8] The E_0 and E_d values of ceramic PT correspond fairly well with the results for our MOCVD PT film, but the E_d decrease as a function of x is small for PLZT ceramics (6%) and cannot be convincingly interpreted as a trend due to the error in these measurements. The unclear modification of E_d for PLZT as a function of the x ratio might be due to an effect of the La dopant or to the correction for surface roughness in the measurements. Similar conclusions can be drawn for PLT sol–gel films,[10] which showed no consistent variation for E_d and/or E_0 as a function of La content. However, our results for MOCVD PZT films clearly show (Fig. 3) a definite decrease in E_d with increasing Zr content. Wemple and DiDomenico[23] noted that E_d was roughly constant (around 23 eV) for most oxides and oxygen–octahedra ferroelectrics, although the trend could not apply to lead-based ferroelectrics as lead does not have a d band, which was used for their classification.[25] Recent calculations by Robertson[26] indicate that states derived from the Pb^{2+} ions enter differently into the conduction bands of PT and PZ, which might account for the smaller interband transition in PZ.

TABLE VII. Reported dispersion parameters for ceramics.

Sample	E_0 (eV)	E_d (eV)	Reference
PLZT (8/90/10)	6.26	28.0	
PLZT (8/80/20)	6.11	28.1	
PLZT (2/65/35)	5.85	27.8	8
PLZT (16/40/60)	5.89	28.9	
PLZT (8/10/90)	5.59	29.4	
PLZT (0/0/100) = PT	5.59	30.0	
$SrTiO_3$	5.8	23.7	23
$BaTiO_3$	5.8	24.5	23
$PbTiO_3$	5.6	29.6	23

C. Waveguide experiments

Light was coupled into rhombohedral PZT layers by 633 nm prism coupling using a rutile prism. Two transverse electric (TE) modes, TE_0 and TE_1, were found to be excitable in a 700 nm thick PZT ($x = 0.6 \pm 0.1$) layer. From the incoupling angles, assuming a homogeneous PZT-core layer and inserting $n_{\text{prism}} = n_c = 2.872$ and $n_{\text{substrate}} = n_{\text{STO}} = 2.389$ and a refractive index $n_{\text{layer}} = 2.505$, a layer thickness $d_{\text{layer}} = 705 \pm 5$ nm could be calculated. This corresponds well with $n_{\text{layer}} = 2.50 \pm 0.01$ and $d_{\text{layer}} = 700 \pm 10$ nm determined by ellipsometry. It should be noted that, because of the relatively low modal field at the outside regions of the PZT-core layer, the coupling angles are very insensitive to the potential presence of a thin interface layer or somewhat lower refractive index and the 1 nm rms surface roughness.

Because both measurement methods are applying completely different field distribution inside the PZT layer, this good correspondence indicates good thickness homogeneity of the PZT core layer. TM light could not be coupled into the films by prism coupling, although the TM_0 and TM_1 modes are accessible using a TiO_2 prism. Similar difficulties were reported for MOCVD PZT films on STO.[11,12] We ascribe this to an insufficient coupling strength as a result of surface roughness, although the rms roughness is only 1 nm for these films. The small dimensions of the substrate (1 by 1 cm) did not allow for quantitative loss measurements of the TE modes. By visual inspection (microscope), strong bulk scattering could be observed in the PZT layer outside the propagating beam area.

IV. CONCLUSIONS

Optical characterization was carried out on PZT films grown by MOCVD on STO, structures of interest for future optical–modulator applications. The top roughness of the PZT films was within the requirements for waveguiding, and two TE modes were coupled in a 700 nm film. For applications, poling of the films might decrease the bulk scattering, which appeared high by visual inspection. The refractive-index dispersion was measured from 1.55 eV (800 nm) to 3.72 eV (333 nm) by ellipsometry and reflectivity, as a function of composition. A Cauchy extrapolation was used to estimate the refractive index down to 0.62 eV (2000 nm). It indicates that the refractive index is close to linear in x, not only at 633 nm, as shown in previous reports, but also up to

2000 nm. The refractive-index determination is thus a convenient measure of composition. The absorption edge is insensitive to composition, and is located at 3.6 ± 0.1 eV (340 ± 10 nm). This is in good agreement with earlier results on ceramics. The interband absorption-strength parameter E_d, extracted from a Wemple–DiDomenico fit to the refractive-index dispersion $n(E)$, decreases nearly linearly from PT to PZ. It is the composition dependence of E_d, rather than that of the average interband gap E_0, which is the dominant factor in the composition dependence of $n(E)$. This is an unusual behavior compared to semiconductors and to other oxides. The smaller infrared refractive index of PZ arises from the smaller E_d for this material.

ACKNOWLEDGMENTS

This project is supported by STW (Dutch Technology Foundation). The authors acknowledge Paul Hageman for his suggestions and Richard Zallen for his very helpful comments and for calling our attention to Refs. 23–26. Paul Lambeck and Henck van Wolferen are acknowledged for their support with the prism-coupling measurements. J. Robertson is acknowledged for making his PZT-band-structure calculations available to them.

[1] R. W. Schwartz, P. C. McIntyre, Y. Miyasaka, S. R. Summerfelt, and D. Wouters (Editors), Ferroelectric Thin Films VIII, Boston, MA, Mater. Res. Soc. Symp. Proc. **596** (2000).
[2] D. K. Fork, F. Armani-Leplingard, and J. J. Kingston, MRS Bull. **21**, 53 (1996).
[3] G. H. Haertling, Ferroelectrics **75**, 25 (1987).
[4] S. L. Chaung, *Physics of Optoelectronic Devices* (Wiley, New York, 1995); C. Buchal and M. Siegert, *Proceedings of the International School of Physics "Enrico Fermi"* (IOS, Amsterdam, 1999) pp. 369–396.
[5] http://www.motorola.com/mediacenter/, press release September 4 2001.
[6] F. Niu, B. H. Hoerman, and B. W. Wessels, Appl. Surf. Sci. **161**, 74 (2000).
[7] C. E. Land, P. D. Thacher, and G. H. Haertling, in *Applied Solid State Science: Advances in Materials and Devices Research 4*, edited by R. Wolfe (Academic, New York, 1974), pp. 137–233; G. H. Haertling, Ferroelectrics **131**, 1 (1992).
[8] P. Thacher, Appl. Opt. **16**, 3210 (1977).
[9] C. H. Peng, J.-F. Chang, and S. Desu, Mater. Res. Soc. Symp. Proc. **243**, 21 (1992).
[10] S. Bhaskar, S. B. Majumder, M. Jain, P. S. Dobal, and R. S. Katiyar, Mater. Sci. Eng., B **87**, 178 (2001).
[11] C. M. Foster, G.-R. Bai, R. Csencsits, J. Vetrone, R. Jammy, L. A. Wills, E. Carr, and J. Amano, J. Appl. Phys. **81**, 2349 (1997).
[12] C. M. Foster *et al.*, J. Appl. Phys. **78**, 2607 (1995).
[13] M. P. Moret, J. J. Schermer, F. Tichelaar, E. Aret, and P. R. Hageman, J. Appl. Phys. (submitted).
[14] F. Gervais, in *Handbook of Optical Constants of Solids II*, edited by E. D. Palik (Academic, Boston, MA, 1991), pp. 1035–1047.
[15] M. P. Moret, M. A. C. Devillers, A. R. A. Zauner, E. Aret, P. H. Hageman, and P. K. Larsen, Integr. Ferroelectr. **36**, 265 (2001).
[16] J. D. Klein and S. L. Clauson, Mater. Res. Soc. Symp. Proc. **361**, 147 (1995).
[17] X. Meng, Z. Huang, H. Ye, J. Cheng, P. Yang, and J. Chu, Mater. Res. Soc. Symp. Proc. **541**, 723 (1999).
[18] A. Deineka, L. Jastrabik, G. Schuneck, and G. Gerlach, Ferroelectrics (to be published).
[19] D. R. Uhlmann, G. Teowee, J. M. Boulton, S. Motakef, and S. C. Lee, J. Non-Cryst. Solids **147&148**, 409 (1992).
[20] S. Trolier-McKinstry, H. Hu, S. B. Krupanidhi, P. Chindaudom, K. Vedam, and R. E. Newnham, Thin Solid Films **230**, 15 (1993).
[21] B. Noheda, J. A. Gonzalo, L. E. Cross, R. Guo, S.-E. Park, D. E. Cox, and G. Shirane, Phys. Rev. B **61**, 8687 (2000).
[22] I. Boerasu, M. I. Vasilevskiy, M. Pereira, M. F. Costa, and M. J. M. Gomes, Ferroelectrics (to be published).
[23] S. H. Wemple and M. DiDomenico, Phys. Rev. B **3**, 1338 (1971); S. H. Wemple, *ibid.* **7**, 3767 (1973); M. DiDomenico and S. H. Wemple, J. Appl. Phys. **40**, 720 (1969); S. H. Wemple, J. Chem. Phys. **67**, 2151 (1977).
[24] D. J. Chadi and M. L. Cohen, Phys. Lett. **49A**, 381 (1974).
[25] S. H. Wemple and M. DiDomenico also use their (E_0, E_d) values to classify materials as "covalent type" and "ionic type." Using their system, PT is covalent and PZ is ionic, even though both solids are oxides with perovskite-based structures and are usually considered to be ionic.
[26] J. Robertson (unpublished).